The Debye Method is Used to Create 3D Structure Models of Electroactively Transformed Microcrystalline Cellulose

Ali M. Ahmed[1*], Qasim Shakir Kadhim[2], Ibrahim A. Ali[3]

Abstract

In this paper, we carried out the XRD results and 3D structural models of short-range order of amorphous cellulose obtained by ball milling of microcrystalline cellulose. The amorphous cellulose has the well-reproducible effect of influence of ozone treatment on its proton conductivity, which allows to use this material as a gas sensor. Calculation of the quantitative characteristics of the short-range order (radii of coordination spheres and their dispersions, coordination numbers) of amorphous cellulose was carried out from distribution pair functions curve by using the Finback-Warren method. The space atoms configurations was carried out by Debye method. After that, the models were distorted by converting into packages disoriented relative to each other layers. The X-Ray diffraction patterns were calculated for 3D models and compared with experimental curves.

Key Words: Microcrystalline Cellulose, Amorphous Cellulose, XRD Methods, 3D Structural Models, Finback-Warren Method, Debye Method.

DOI Number: 10.14704/nq.2021.19.6.NQ21059 **NeuroQuantology 2021; 19(6):01-07**

Introduction

Microcrystalline cellulose studies A large number of works are devoted to various kinds of impacts and modifications. Interest in these objects, in particular, is due to the effects of charge transfer and redistribution of space charge in composite materials based on a matrix of microcrystalline cellulose subjected to mechanical destruction (Pikulev, 2012, V, Pikulev V. B2014). The effect of changes in conductivity in a cellulose matrix containing bound water as a result of exposure to ozone with a concentration from ppb units can be explained by the generation of an additional amount of protons during the decay of ozone molecules on the surface and in the pores of amorphous cellulose. In (Pikulev, V.B, 2015) it was suggested that this the effect is associated both with the generation of an additional amount of hydroxonium ions on the network of water bridges, and with an increase in the concentration of water in the pores, as well as with the neutralization of excess protons during the dissociation of the ozone molecule near the negatively charged copper electrode. By changing the structure of cellulose at micro- and nano-levels, it is possible to reach an effective sensor element operating in the current range above 10^{-8} A, which is quite enough to develop inexpensive and compact measuring devices. It is equally important that the cellulosic matrix itself is sufficiently inert with respect to the ozone effect. For a number of cellulose-based composites, an increased concentration of protons (hydroxonium ions) is characteristic, which determines the specific optical properties of these materials.

Corresponding author: Ali M. Ahmed
Address: [1*]Al-Esraa University College, Iraq; [2]College of Basic Education, University of Babylon, Iraq; [3]Uruk University, Iraq.
[1*]E-mail: ali.m.alshammary@gmail.com
Relevant conflicts of interest/financial disclosures: The authors declare that the research was conducted in the absence of any commercial or financial relationships that could be construed as a potential conflict of interest.
Received: 20 March 2021 **Accepted:** 10 May 2021

As an example, one can cite the stable luminescence of silicon nanoparticles placed in the cellulose matrix, as well as the luminescence of a number of organic luminophores, similar to their luminescence in aqueous solutions (L.A. Aleshina, V.A. Gurtov, N.V. Melekh, 2014). In general, despite the wide practical application of cellulosic materials, there are no systematic studies of the structure of modified microcrystalline and amorphous cellulose and mutual and its structure and properties. Currently, there is an increased interest in the development of new polyfunctional materials based on nanostructured cellulose (Okahisa, Y., Yoshida, A., Miyaguchi, S, 2009). In this paper, the grinding of microcrystalline cellulose (MCC) with a particle size of less than 40 microns, a water content of about 5 wt.%. held in the planetary micromill Pulverisette 7 premium line. A 20 ml agate grinding bowl and ø5 mm isagat grinding balls were used. The volume of the original powder was 9 ml (2.7 g). The powders were ground from 1 to 6 hours.

Experimental Part

After each hour of grinding, the structural state of the cellulose was analyzed by X-ray diffraction and IR spectroscopy. Analysis of the IR absorption spectra of MCCs and grinding products suggests that mechanical destruction leads to the destruction of intramolecular and intermolecular hydrogen bonds, since the peaks of free alcohol groups were changed (Marechal Y., Chanzy H.,200). And also observed an increase in the maximum of 898 cm $^{-1}$ and a decrease in the peak of 1433 cm $^{-1}$, indicating an increase in the amount of the amorphous phase as a result of grinding. The X-ray diffraction of the samples was carried out on an automated diffractometer DRON-6.0 for MoKα– and FeKα – radiation in symmetric geometry for transmission and reflection. The X-ray diffraction pattern of the initial MCC (Fig. 1a) is characteristic of an amorphous-crystalline material. The calculations of the degree of crystallinity, performed by the well-known method (Pikulev V.B., Loginova S.V., Gurtov V.A, 2012), give values of 75 ± 5%, which is consistent with the data obtained from the analysis of the IR spectra of the MCC by the Nelson-O'Connor method. The atomic structure of the MCC can be described in part of model Ib with antiparallel arrangement of cellulose chains. The unit cell period values specified by the Rietveld method are: a = 0.787 nm, b = 0.815 nm, c = 1.034 nm, the monoclinic angle is 96.3 ° (the values of the uncertainty factors were: weight profile R_{wp} = 8.54%, profile R_p = 6, 10%) (Pikulev V.B., Loginova S.V., Gurtov V.A, 2012). The curves of the distribution of the scattering intensity of the samples of the initial MCC and cellulose that has undergone mechanical grinding for 1 and 6 hours are shown in Fig. 1a and 1b, respectively.

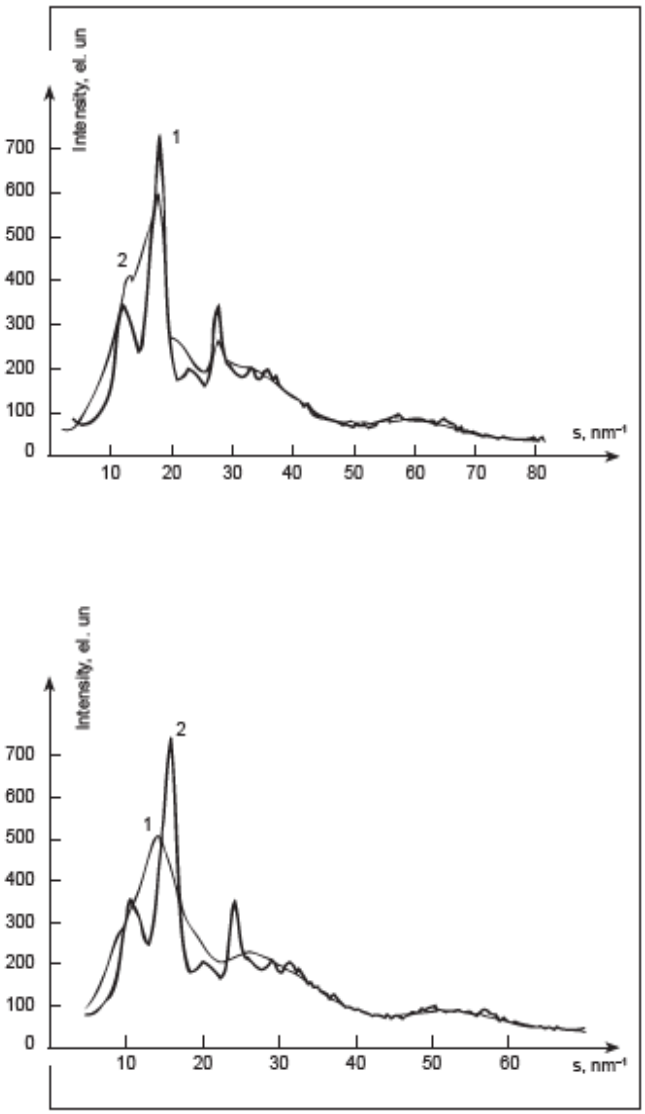

2

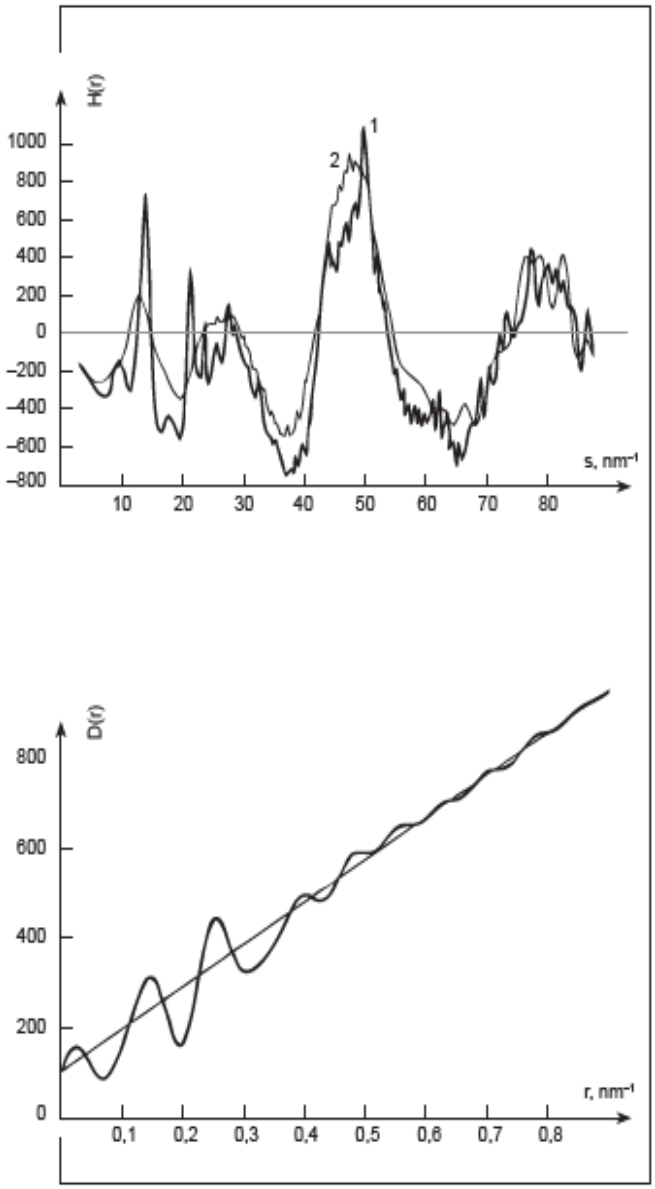

Fig. 1. Comparison of the scattering intensity distribution curves the initial MCC (1) and grinding for: a) 1 hour and b) 6 hours, obtained in the geometry of the passage; c) s-weighted interference functions H (s) of the original MCC (1) and a sample of cellulose after 6 hours of grinding; d) the distribution curve of the paired functions D (r) of the ground pulp

As follows from fig. 1a, on the radiograph of the sample after the first in the first hour of grinding, the traces of the three strongest reflections of crystalline cellulose I are clearly visible. The degree of crystallinity of this sample, estimated by the Segal method (Terinte, N., Ibbett, R., 2011), decreases by 35%. The crystallite size in the [100] direction calculated from the reflection width (200) is 3 ± 0.5 nm, the size of the CSR in the same direction in the original MCC is 5.5 ± 0.5 nm. Estimation of the length of ordered regions allows one to say that it decreases by 3 nm and becomes equal to 5.5 ± 0.5 nm. Thus, after one hour of grinding, the thickness and length of the ordered regions of the elementary fibrils decrease by approximately 3 nm. Already after the three-hour destruction of the MCC, the diffraction pattern on the sample under study, it becomes similar to the diffraction pattern of the amorphous material (Fig. 1b). The subsequent grinding (up to 6 hours) does not lead to a change in the shape of the scattering intensity distribution curve: an x-ray of pulp ground for 3 hours coincides with radiographs of cellulose ground for 6 hours. Comparison of the scattering intensity distribution curve of the original MCC and radiographs of 6 hours of grinding suggests that the structure of the amorphous component of MCC and pulverized cellulose is different. Comparison of s-weighted interference function curves The scattering of the initial and ground MCC (Fig. 1c) shows that the curve of the ground pulp is more blurred. The intense peak located at the length of the diffraction vector s = 16.0 nm^{-1} is strongly blurred. The position of this peak corresponds to the distance between neighboring chains in the unit cell, namely, between the average ring planes in the neighboring chains of the cellulose Ib model with an anti-parallel arrangement of cellulose chains equal to 0.392 nm (half of the period of the unit cell). Thus, the blurring of this peak indicates the disorientation of the chains during the grinding process. Consequently, there is a gap and a change in the lengths of hydrogen bonds between the macromolecules of cellulose. From the distribution curves of the pairwise functions (Fig. 1c), Finback – Warren methods (Aleshina LA, Loginova S.V., 2005) determine the short-range order characteristics (radii of the coordination spheres r_{ij}, their smearing σ_{ij} and coordination numbers N_{ij}) of amorphous cellulose powder ground during 6 h. The values of the radii of the coordination spheres in the first approximation were set based on relevant data calculated for crystalline Ib cellulose with antiparallel arrangement of cellulose chains. Table 1 presents the results of calculations of characteristics near order in comparison with the corresponding data for the model. The calculation for the model is made with and without the contribution of the spheres C-H and O-H. Since the pair of atoms of different types contribute to the coordination spheres, the average weight radii and the total coordination numbers of the combined spheres were calculated, taking into account that the area under the maximum of the distribution curve of pair functions (Fig. 2d) should be equal to the sum of the maximum areas formed by each pair atoms. From the analysis of the data presented in Table 1, it

follows that taking into account the contribution of C – H and O – H bonds in the calculation for the model leads to a decrease in the radius of the coordination sphere to 0.135 nm and an increase in the coordination la to 1.40. The radius of the coordination sphere C-O and the number of Atoms on it, calculated from the experiment, coincide with the corresponding data for the model. The increase in the radius of the first C-C sphere may be due to the formation of cellulose chains, inevitable with mechanical destruction. The coordination number on the C-C sphere coincides with the data for models. When spheres are combined into the first O – O sphere with a radius of 0.226 nm, pairs of atoms C – H and O – H contribute. As a result, the weight-average radius of the combined coordination sphere decreases to 0.212 nm, and the coordination number increases to 1.62 at. Determined The experimental value of the radius of the first O – O sphere within the experimental error coincides with the calculations for the model

Table 1. The results of the calculation of the characteristics of the near order of pulp, ground for 6 hours, in comparison with the corresponding experimental data

type of sphere	r_{ij}, nm	σ_{ij}, nm	N_{ij}, *at,*
C-O(1)	0,137	0,022	*1,3*
C-C(1)	0,157	0,027	*1, 7*
O-O(1)	0,216	0,015	*0,8*
C-O(2)	0,238	0,043	*2,2*
C-C(2)	*0,259*	*0,001*	*7,6*

$$\Delta r_{ij} = \pm 0.005nm, \Delta\sigma_{ij} = \pm 0.005nm, \Delta N_{ij} = \pm 0.1at$$

One number on the O-O sphere for ground pulp equal to 0.8 at., which is half the value calculated for the model. Moreover, this value is twice the number of oxygen atoms separated from another oxygen atom at a distance of 0.226 nm in the model under consideration. This difference may be due to C-H deformation and O-H chains. . The sufficiently strong deformation of cellulose fragments is also indicated by the large values of the dispersions of the radii of all coordination spheres. The radius and number of atoms on the second C-O sphere are equal to the corresponding values calculated for the model. The number of atoms on the second C – C coordination sphere is too high compared to the data for the crystalline data for the Iβ cellulose model with antiparallel arrangement of cellulose chains.

Iβ with antiparallel location of chains			Iβ with antiparallel arrangement of the flail. (without the contribution of C-H and O-H spheres)		
r_{ij}nm	σ_{ij}nm	$N_{ij}at$	r_{ij} nm	σ_{ij}nm	$N_{ij}at$
0,135	0,001	1,40	0,142	0,001	1,17
0,152	0,001	1,70	0,151	0,001	1,67
0,212	0,003	1,62	0,226	0,000	0,40
0,239	0,002	1,97	0,239	0,001	1,96
0,254	0,001	3,16	0,249	0,001	1,67

Modifications, since the calculations did not take into account ten contribution of subsequent spheres that overlap with this one. Building possible models describing short range ordering in amorphous cellulose, was carried out by the Debye method. Initially space atomic configurations were formed within models of randomly disordered undistorted clusters, i.e., clusters formed by translation unit cell (Aleshina L. A., Melekh N. V. 2005). Building possible models describing short range ordering in amorphous cellulose, was carried out by the Debye method. Initially space atomic configurations were formed within models of randomly disordered undistorted clusters, i.e., clusters formed by translation unit cell (Aleshina L. A., Melekh N. V. 2005). As a starting element unit cell were selected elementary cell Iα, which accounts for one cellulose a chain (Aabloo A., French A.D., 1994), and a unit cell of cellobiose (Melekh N.V., Aleshina L.A., 2012). As part of this approach, more than a dozen models were built. In view of the fact that, as a result of pulverization, the sizes of ordered areas decrease, clusters of small sizes were formed. So for models built on the basis of cellulose Iα, the linear dimensions of the clusters were no more than 3–4 nm. A further increase in size led to the appearance of intense reflections on theoretical radiographs, which is not typical for radiographs of amorphous material. Further, the calculation of the intensity distribution curves scattering formula Debye:

$$I(s) = \frac{1}{N_{\emptyset}}\left[\sum_{i=1}^{N} f_i^2 + 2\sum_{i}^{N-1}\sum_{j=i+1}^{N}\frac{1}{2} * \left[f_i f_j^* + f_i^* f_j\right] * \frac{\sin(s.r_{ij})}{s.r_{ij}} \exp\left(-0.5\sigma_{ij}^2 s^2\right)\right]$$

Where f_i, f_j - are the atomic scattering functions of the i-th and j-th atoms;
N - is the number of atoms in the considered configuration;
σ_{ij} - is the dispersion of interatomic distances relative to the average value of r_{ij};
N_f - is the number of formula units in the configuration (Aleshina L. A., Melekh N.V. 2005).
Then the theoretical intensity distribution curves the scattering values for undistorted clusters were compared with an experimental X-ray diffraction pattern of amorphous cellulose. To determine the degree of discrepancy between these curves, the profile uncertainty factor R_p was calculated. The lowest value of the profile uncertainty factor (10.5%) was obtained by comparing the experimental scattering intensity distribution curve with a diffraction pattern built for a cellobiose cluster formed by translating the unit cell of the crystal modification once along the x axis, twice along the y axis and three times along the z axis (cluster size 1a ×2b × 3c where a, b and c are the periods of the unit cell of cellobiose (Fig. 2 a).

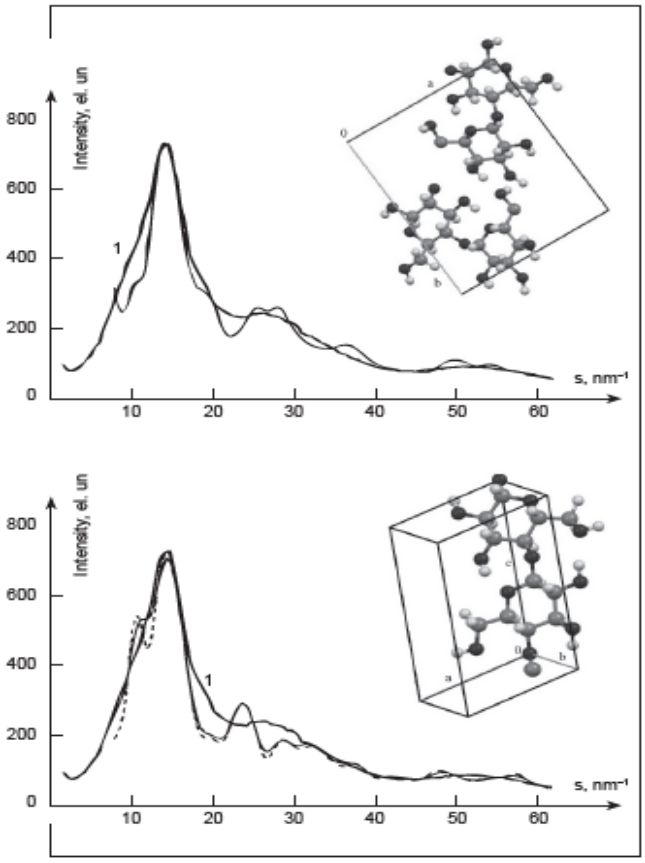

Fig. 2. The scattering intensity distribution curves of amorphous pulp (1) and clusters based on unit cell: a) cellobiose, cluster size 1a, 2b, 3c; b) Iα, dimensions - 3a × 2b × 2c (solid line) and 4a × 2b × 2c. Types of elementary cells of cellobiose (z axis is directed deep into the picture) and cellulose Iα.

Cellobiose molecules do not form chains extended along the z axis, as is the case in cellulose. The unit cell has two molecules, each of which consists of two glucose residues, like the elementary unit of cellulose. Therefore, it is the absence of translational symmetry along the z axis, as well as features in the arrangement molecules in the unit cell allow a good agreement between the theoretical curve and the experimental x-ray. This is confirmed by the results of IR-spectroscopy, according to which six-hour grinding does not lead to such a significant destruction of the material. The unit cell of the Iα cellulose accounts for one chain. When building clusters based on this modification, the best values of the core uncertainty factor (11.5%) were achieved for a cluster with dimensions of 3a × 2b × 2c. A comparison of the theoretical X-ray pattern for a cluster with an experimental curve is shown in Fig. 2b. The presence of a narrow maximum at the modulus of the diffraction vector s ~ 23.5 nm^{-1}, as well as the appearance of a peak in the range from 10 to 13 nm^{-1} on the I (s) curve, suggests that the degree of ordering of the model cluster is higher than that of amorphous pulp. A subsequent increase in the number of translations of the unit cell along the x axis (Fig. 2b) leads to an increase in the maximum located at a value of s ~ 11.5 nm^{-1}. It should be noted that when choosing any of the four well-known models of the structure of cellulose Iβ as the initial unit cell, the values of the profile factors of uncertainty were within 20–25%. On the basis of which it was concluded that the models based on the crystalline modification of cellulose Iβ are bad describe the structure of amorphous cellulose. This is explained by the fact that the unit cell of the Iβ modification contains two molecular chains that are strictly ordered relative to each other. And the results of the radiographic experiment show that as a result of mechanical destruction, the chains are disoriented relative to each other. It is considered (L.A. Aleshina, V.A. Gurtov, N.V. Melekh, 2014) that if the value of the profile factor is unremarkable fidelity at this stage of work is less than 10–15%, then the model can be used at the next stage of modeling: the construction of distorted clusters. The essence of building models of distorted clusters is described in detail in (Aleshina L.A., Melekh N.V., 2005). Initially obtained in the previous step, the cluster on the cell-based Iα unit cell was transformed into packages consisting of three or four layers with dimensions of 1a × 2b × 2c. The total number of atoms in a cluster was 504 or 672 atoms, depending on the number of layers forming it. Then,

these packets were distorted by shifting, turning the layers relative to each other, changing the distance between the layers. Distortions were introduced into the cluster gradually to achieve a better agreement between the theoretical and experimental radiographs. When constructing distorted lattice regions, a check was performed on the "intersection" of atoms by calculating the shortest distances between them. In the event of such detection, this cluster was not further considered, i.e., only those clusters were involved in further calculations, for which the composition of $C_6H_{10}O_5$ was maintained. Smaller values of the profile uncertainty factor were obtained by introducing the following distortions into a model cluster consisting of four layers with dimensions of 1a × 2b × 2c: the distances between the grids were varied in accordance with the Gaussian distribution for the average distances from 0.7 to 0.85 nm, while the dispersions were equal to zero; the layers were turned around the x axis passing through the first atoms we are in adjacent layers, at angles from 0 ° to 10 ° with a dispersion of 5 °; the layers were shifted at distances from -0.05 nm to 0.5 nm in accordance with the Gaussian distribution with a given dispersion (0.5 nm). The above violations of the interference conditions lead to a blurring of the peak (Fig. 3) with the modulus of the diffraction vector s ~ 23.5 nm^{-1}. Although the cluster is formed by four layers, a peak at s ~ 11.5 nm^{-1} is not observed. The agreement of the model curve with the experimental distribution of the scattering intensity improves (Fig. 3): distortion of the cluster leads to a blurring of the first and second maximum, but the complete coincidence of the curves I (s) ranges from 20 to 35 nm^{-1} cannot be achieved. Calculate tannoy value of the profile factor of uncertainty is 8.8%. A comparison of the experimental X-ray diffraction patterns of amorphous cellulose with the corresponding curves for distorted clusters showed that increasing the rotation angle of the layers along the x axis more than 15 ° does not improve the coincidence of the curves.

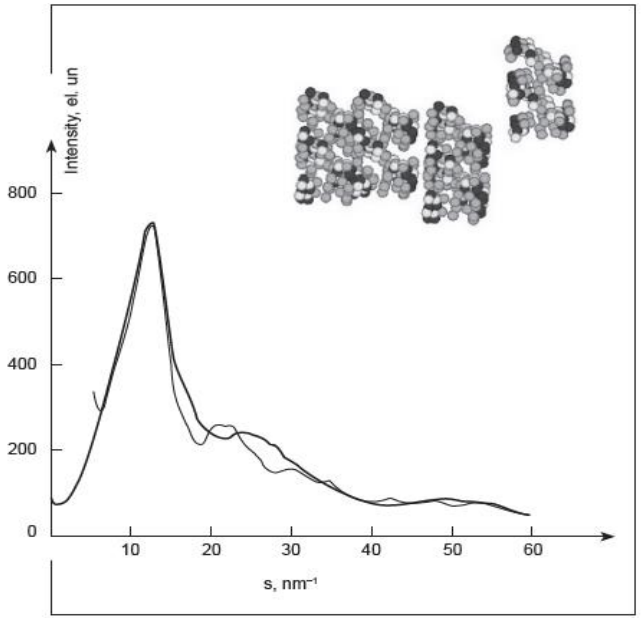

Fig. 3. Comparison of the experimental distribution curve of the scattering intensity (1) and the theoretically calculated for a distorted cluster consisting of four layers with dimensions 1a × 2b × 2c, built on the basis of elementary Noah cell pulp Iα. Kind of a distorted cluster.

Conclusion

Thus, as a result of the mechanical destruction of microcrystalline cellulose, the sizes of coherent scattering regions gradually decrease. Already after the first hour of grinding, the thickness and length of the ordered regions of elementary fibrils decrease by approximately 3 nm compared with the corresponding values of 5.5 nm.and 8.5 nm for the original microcrystalline cellulose. The degree of crystallinity becomes equal to 40%. After three hours of mechanical destruction of the MCC, its diffraction pattern becomes similar to the diffraction pattern of amorphous material, the form of which does not undergo changes up to 6 hours of grinding. During the grinding process, cellulose chains are deformed, as a result of which the bond lengths in cellulose molecules, including hydrogen bonds, change. connections within and between adjacent macromolecules. In the model of randomly disoriented clusters, the spatial configuration of atoms in the short-range ordering of amorphous cellulose can be described by small (up to 32 formula units) distorted clusters with sizes not exceeding 3 nm. The arrangement of single cellulose chains ~ 2.1 nm long in these clusters differs from that in the crystalline modifications of cellulose I: the macromolecules are displaced relative to each other and disoriented into small angles whose values do not exceed 15°.

References

Aabloo A, French A.D. The tentative potential of crystal structure Iα crystal structure. *Macromolecular Chemistry Theory and Simulating* 1994; 2: 119-125.

Aleshina LA, Loginova SV. The short-range order in the powder of amorphous anodic yttrium oxide. *Crystallography* 2003; 48(4): 583–587.

Aleshina LA, Melekh NV, Fofanov AD. Investigation of the structure of cellulose and lignins of various origin. *Chemistry of plant raw materials* 2005; 3: 31–59.

Maréchal Y, Chanzy H. The hydrogen bond network in Iβ cellulose as observed by infrared spectrometry. *Journal of molecular structure* 2000; 523(1-3): 183-196.

Melekh NV, Aleshina LA. Refining the atomic structure of cellobiose powder by the Rietveld method. *Scientific notes of Petrozavodsk State University. Series: Natural and Technical Sciences* 2012; 6(127): 101– 105.

Okahisa Y, Yoshida A, Miyaguchi S, Yano H. Optically transparent wood–cellulose nanocomposite as a base substrate for flexible organic light-emitting diode displays. *Composites Science and Technology* 2009; 69(11-12): 1958-1961.

Pikulev V. B., loginova S.V., Prokopovich P.F.2014, Gurtov V.A. - Q.P1–26.

Pikulev VB, Prokopovich PF, Gurtov VA. Effect of Ozone on Charge Transfer in Microcrystalline Cellulose, *Uch. notes of Petrozavodsk State. university* 2015; 2(148): 77–81.

Pikulev VB, Loginova SV, Gurtov VA. The influence of natural and stimulated oxidation on luminescent properties of silicon-cellulose nanocomposites. *Technical Physics Letters* 2012; 38(8): 723-725.

Pikulev V, Loginova S, Gurtov V. Luminescence properties of silicon-cellulose nanocomposite. Nanoscale research letters 2012; 7(1): 1-6.

Aleshina LA, Gurtov VA, Meleh NV. *Structure and physico-chemical properties of the cellulose and nanocomposites based on them.* Petrozavodsk State University, Russia 2014: 240.

Terinte N, Ibbett R, Schuster KC. Overview on native cellulose and microcrystalline cellulose I structure studied by X-ray diffraction (WAXD): Comparison between measurement techniques. *Lenzinger Berichte* 2011; 89(1): 118-131.

Abdulrazzak FH, Abass AM, Alkaim AF, Hussein FH. Comparison between chemical vapor deposition and flame fragments deposition techniques for synthesizing carbon nanotubes. *NeuroQuantology* 2020; 18(4): 5-10.